

Supporting Information

Optical Anisotropy and Sign Reversal in Layer-by-Layer Assembled Films from Chiral Nanoparticles

Zhumei Liang^{1,2,3} Kalil Bernardino,⁴ Jishu Han,^{1,2} Yunlong Zhou^{1,2}, Kai Sun⁵,
André F. de Moura^{*,4} Nicholas A. Kotov^{1,2,3,5,6*}

¹Department of Chemical Engineering, University of Michigan, Ann Arbor, Michigan, 48109;

²Biointerfaces Institute, University of Michigan, Ann Arbor, Michigan, 48109;

³School of Chemistry and Chemical Engineering, State Key Laboratory Metal Matrix Composites, Shanghai Jiao Tong University, 800 Dongchuan Road, Shanghai, China, 200240;

⁴Department of Chemistry, Federal University of São Carlos, São Carlos, Brazil, 13565-905;

⁵Department of Materials Science and Engineering, University of Michigan, Ann Arbor, Michigan 48109;

⁶ Michigan Center for Integrative Research in Critical Care, Ann Arbor, MI, USA

Corresponding authors: Nicholas A. Kotov: kotov@umich.edu
André F. de Moura: moura@ufscar.br

The size of CdS NPs was determined by TEM measurements, as shown in Figure S1, the size of CdS-D and CdS-L is about 3 nm.

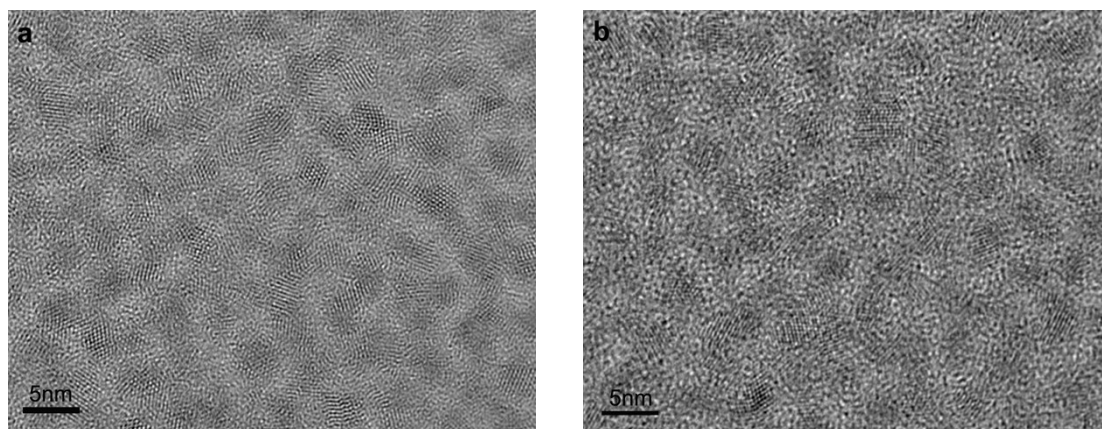


Figure S1. TEM images of (a) CdS-D and (b) CdS-L

Additional data on LBL deposition of film

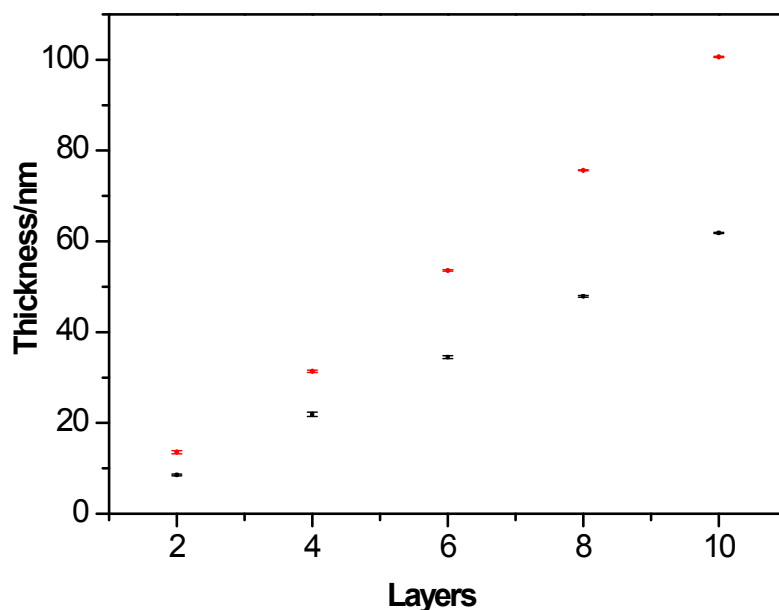


Figure S2. Thickness dependence of D_n (black) and L_n (red) films on number of layers

Calculations of Chiroptical Activity of the Films under assumption that experimentally measure polarization rotation primarily originates from interactions of incident photons with chiral NPs.

From Lambert-Beer's Law, one can define a molar absorption

$$\Delta\varepsilon = \frac{\Delta A}{c \cdot b} \quad (1)$$

Which is independent of the concentration c , expressed in $\text{mol} \cdot \text{L}^{-1}$, and of the pathlength b , expressed in cm. The circular dichroism is defined as the difference $\Delta A = A^D - A^L$, where A^D and A^L are the absorptions of left and right circularly polarized light, respectively. The output of CD spectrometers is usually measured as ellipticity θ (in mdeg), related to ΔA through $\theta \text{ (mdeg)} = 33000 \Delta A$.

In our research, the concentration of CdS NPs in the LBL film can be expressed as

$$c = \frac{N_{NP} / NA}{V_{film}},$$

here N_{NP} is the number of CdS NPs in LBL film, NA is Avogadro constant, V_{film} is the volume of LBL film. For calculating c , we need to know the weight percent of

CdS NPs in LBL film, the density of CdS ($\rho_{CdS}=4.82\text{g/cm}^3$) and PDDA ($\rho_{PDDA}=1.26\text{g/cm}^3$) and the volume of one CdS NPs, which can be calculated by $V_{NP}=\frac{4}{3}\pi R^3$, R can be obtained from TEM images ($R=1.5\text{nm}$, see Figure S1).

The TGA curves of pure PDDA and LBL films were obtained under N_2 flow. The data (wt%=73%) of 600°C was used as the weight percent of CdS NPs in LBL film.

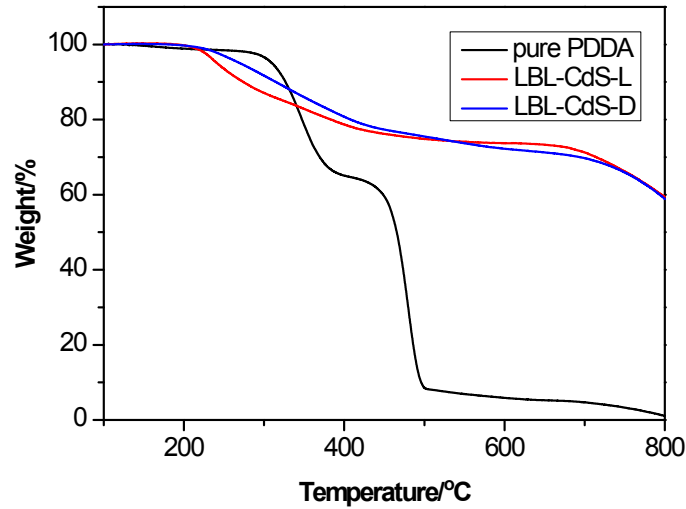


Figure S3. TGA curves of LBL films and pure PDDA under N_2 flow

$$\begin{aligned}
 TGA(\text{wt}\%) &= \frac{M_{NPs}}{M_{NPs} + M_{PDDA}} \\
 &= \frac{\rho_{CdS} \cdot N_{NPs} V_{NP}}{\rho_{CdS} \cdot N_{NPs} V_{NP} + \rho_{PDDA} \cdot V_{PDDA}} \\
 &= \frac{\rho_{CdS} \cdot N_{NPs} V_{NP}}{\rho_{CdS} \cdot N_{NPs} V_{NP} + \rho_{PDDA} (V_{film} - N_{NPs} V_{NP})} \\
 &= \frac{\rho_{CdS} \cdot N_{NPs}}{V_{NP} (\rho_{CdS} - \rho_{PDDA}) + \rho_{PDDA} \frac{V_{film}}{N_{NPs}}} \\
 \therefore \frac{V_{film}}{N_{NPs}} &= \frac{\rho_{CdS} \cdot V_{NP}}{TGA(\text{wt}\%) \cdot \rho_{PDDA}} - \frac{V_{NP} (\rho_{CdS} - \rho_{PDDA})}{\rho_{PDDA}} \\
 &= \frac{4.82 \times \frac{4}{3} \pi \times (1.5 \times 10^{-9})^3}{0.73 \times 1.26} - \frac{\frac{4}{3} \pi \times (1.5 \times 10^{-9})^3 \times (4.82 - 1.26)}{1.26} \\
 &= 34.14 \times 10^{-27} \text{m}^3 \\
 &= 34.14 \times 10^{-24} \text{L}^3
 \end{aligned}$$

$$c = \frac{N_{NP} / NA}{V_{film}} = \frac{1}{34.14 \times 10^{-24} L \times 6.022 \times 10^{23} mol^{-1}} = 0.0486 mol / L$$

The path length of CE measurement in LBL films is 15 or 20 bilayers, but the thickness data listed in Table S1 is the films on silicon wafer substrate, only 15 or 20 layers, so the path length used in equation (1) should be 2 times of the thickness measured by ellipsometer. Figure S4 is SEM images of fracture surface of LBL films at 15 and 20 layers on the silicon substrate.

Table S1. Ellipsometric and SEM thickness of prepared films.

Film/Cycles	Ellipsometer(nm)/SEM(nm)
D ₁₅	115/115.0
D ₂₀	169/177.5
L ₁₅	135/121.6
L ₂₀	187/222.6

So, for D₂₀ at the wavelength of 396nm, $\theta=2.8$ mdeg, $b=169nm \times 2=338nm=338 \times 10^{-7}$ cm, $c = 0.0486$ mol/L

$$\Delta\varepsilon = \frac{\Delta A}{c \cdot b} = \frac{\theta}{33000 \times c \times b} = \frac{2.80368}{33000 \times 0.0486 \times 338 \times 10^{-7}} = 51.7$$

Table S2. $\Delta\varepsilon$ of D₁₅, D₂₀, L₁₅ and L₂₀ at different wavelength.

Film	$\Delta\varepsilon(cm^{-1}M^{-1}) / \lambda$	
D ₁₅	-18.5 /343nm	48.6/396nm
D ₂₀	-12.6 /343nm	51.7/396nm
L ₁₅	54.0/347nm	-41.2/397nm
L ₂₀	71.5/347nm	-95.6/397nm

Table S3. $\Delta\varepsilon$ of some organic molecules and bio-molecules.

Samples	$\lambda(\Delta\varepsilon)$	
Natural products ¹	Dendryphiellin F	257nm(+36.9)/234nm(-19.0)
	Abscisic acid	265nm(+44.3)/233nm(-36.5)

	calycanthine	259nm(+18)/240nm(-20.0)
	quassin	266nm(+10.4)/242nm(-9.5)
	Arnottn II	261nm(-79)/221nm(+39)
	vinblastine	228nm(+31)/214nm(-73.4)
RNA ²	A-form	170nm(-25)/190nm(+33)
	A' -form	170nm(-25)/189nm(+35)
	A-form(A·U) ₂₀	167nm(-39)/187nm(+43)
	A-form(G·C) ₂₀	173nm(-20)/189nm(+47)
DNA ²	A-form	170nm(-25)/190nm(+34)
	B-form	170nm(-15)/190nm(+14)
	B-form(A·T) ₂₀	168nm(-22)/186nm(+25)
	B-form(G·C) ₂₀	174nm(-17)/190nm(+22)

Transition Densities from TD-DFT Calculation of CdS-D.

Details of the calculations are described in the main article. Hydrogen atoms were excluded for better visualization. Red surfaces correspond to regions with electronic density smaller than the ground state whereas while blue surfaces correspond to increased electronic density. All surfaces are plotted with an isovalue of 0.0005 $e/bohr^3$. The names of the bands correspond to those used in the discussion of the experimental circular dichroism spectra (Figure 3 in the main article).

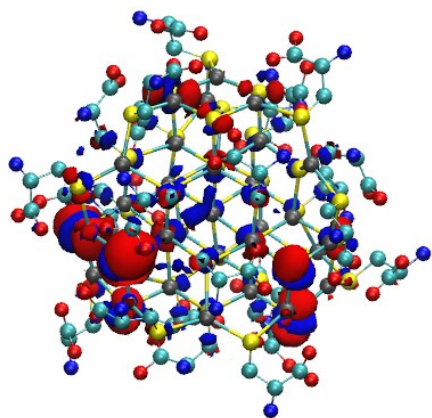


Figure S4 – Transition at $\lambda=382$ nm (ChiNP390 band).

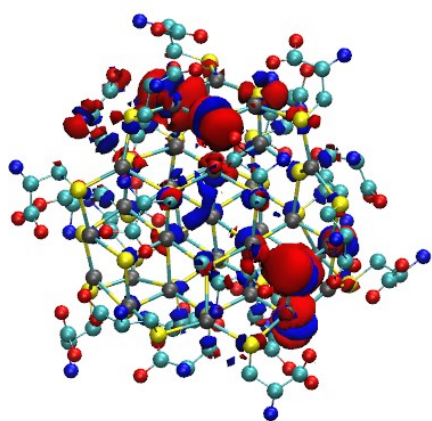


Figure S5 – Transition at $\lambda=380$ nm (ChiNP390 band).

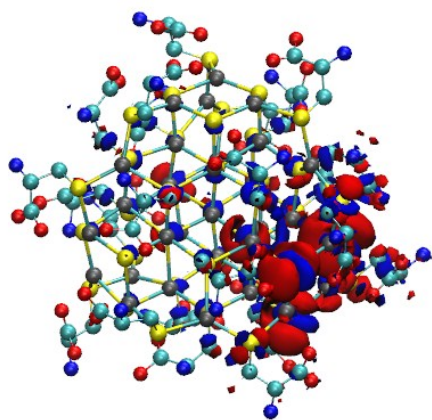


Figure S6 – Transition at $\lambda=374$ nm (ChiNP390 band).

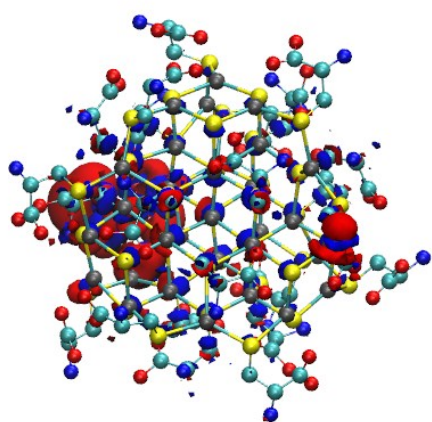


Figure S7 – Transition at $\lambda=346$ nm (ChiNP357 band).

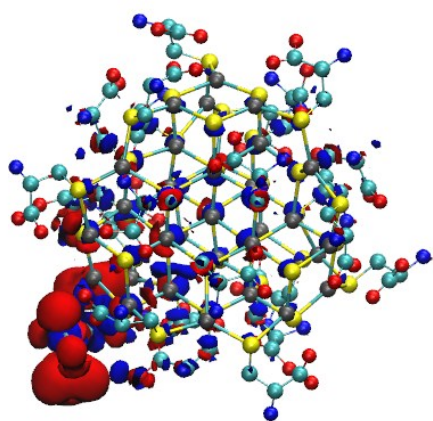


Figure S8 – Transition at $\lambda=345$ nm (ChiNP357 band).

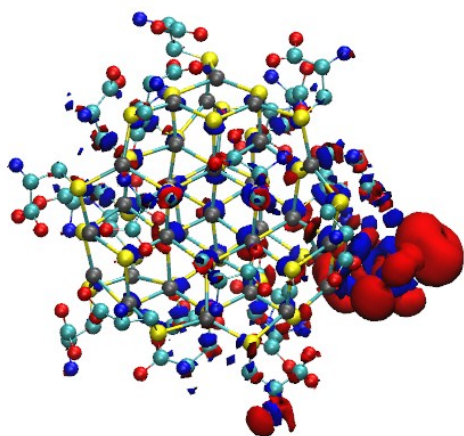


Figure S9 – Transition at $\lambda=341$ nm (ChiNP357 band).

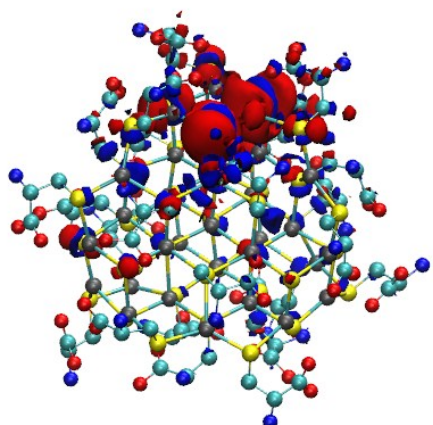


Figure S10 – Transition at $\lambda=306$ nm (ChiNP310 band).

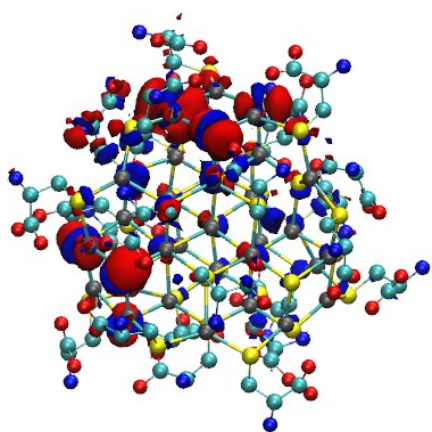


Figure S11 – Transition at $\lambda=304$ nm (ChiNP310 band).

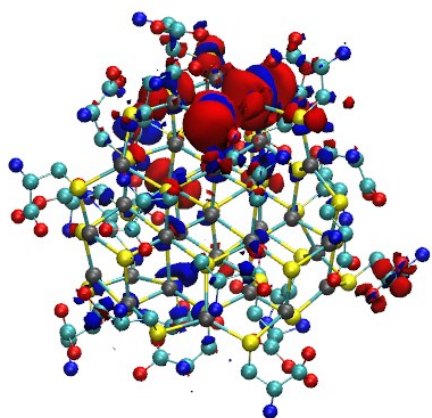


Figure S12 – Transition at $\lambda=302$ nm (ChiNP310 band).

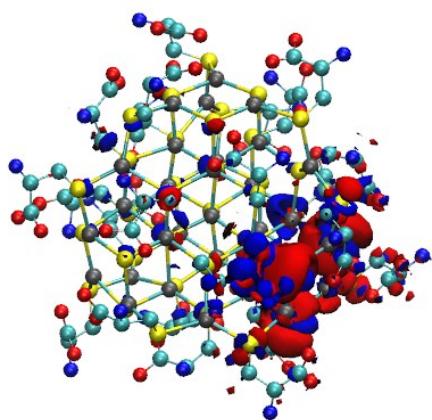


Figure S13 – Transition at $\lambda=300$ nm (ChiNP310 band).

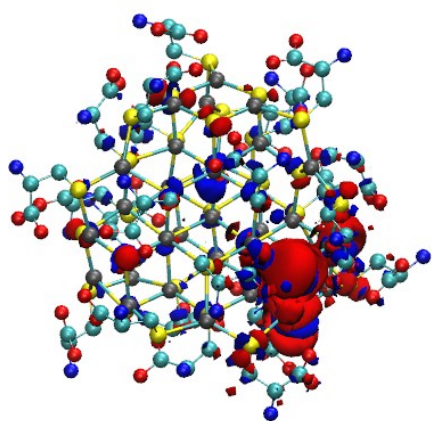


Figure S14 – Transition at $\lambda=299$ nm (ChiNP310 band).

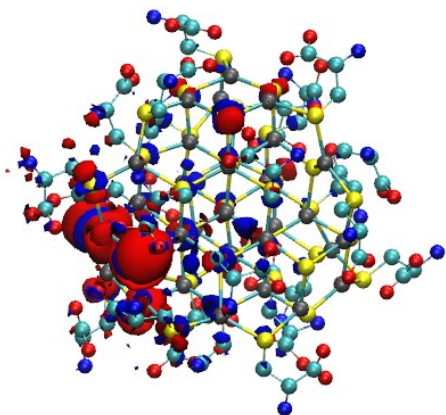


Figure S15 – Transition at $\lambda=293$ nm (ChiNP310 band).

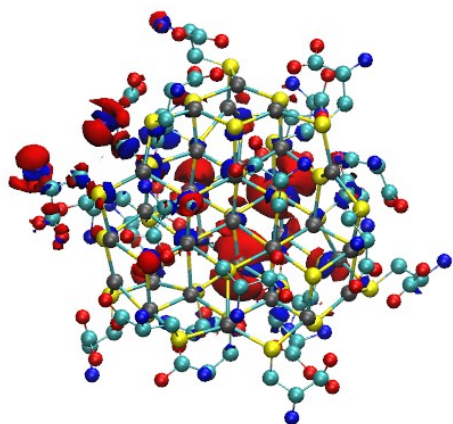


Figure S16 – Transition at $\lambda=292$ nm (ChiNP310 band).

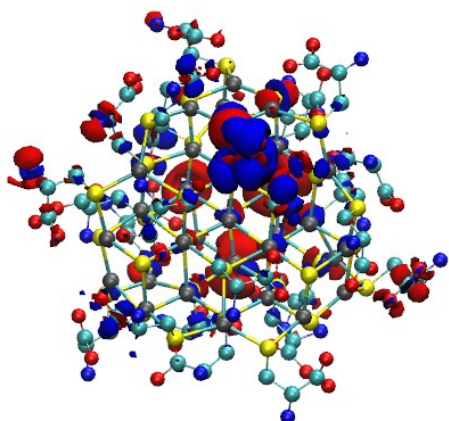


Figure S17 – Transition at $\lambda=290$ nm (ChiNP290 band).

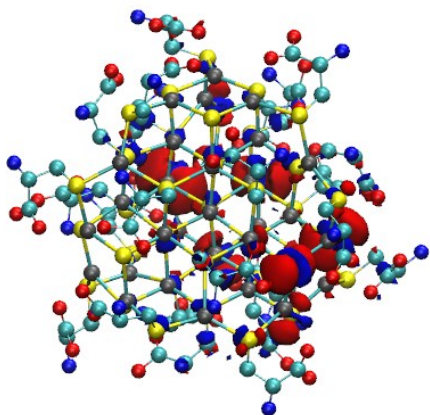


Figure S18 – Transition at $\lambda=289$ nm (ChiNP290 band).

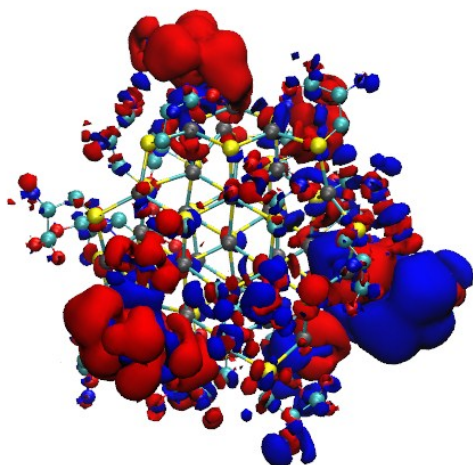


Figure S19 – Transition at $\lambda=281$ nm (ChiNP290 band).

REFERENCES

1. Berova, N.; Bari, L. D.; Pescitelli, G. Application of Electronic Circular Dichroism in Configurational and Conformational Analysis of Organic Compounds. *Chem. Soc. Rev.*, **2007**, 36, 914-931.
2. Rizzo, V.; Schellman, J. A. Matrix-Method Calculation of Linear and Circular Dichroism Spectra of Nucleic Acids and Polynucleotides. *Biopolymers*. **1984**, 23, 435-470.